

X-ray imaging performance of a CdTe photon-counting detector

Junho Lee^a, Seungjun Yoo^a, Seokwon Oh^a, and Ho Kyung Kim^{a,*}

^a Radiation Imaging Laboratory, School of Mechanical Engineering, Pusan Nat'l Univ., Busandaehakro 63beon-gil, Busan 46241

*Corresponding author: hokyung@pusan.ac.kr

***Keywords : photon-counting detectors, detective quantum efficiency, dual energy X-ray imaging**

1. Introduction

X-ray imaging detectors can be categorized into two types based on their operation [1]. The first type is energy-integrating detectors (EIDs), which convert the energy of photons entering the pixel into a signal. The second type is photon-counting detectors (PCDs), which count each photon entering the pixel. PCDs also provide energy-selective images for each energy bin channel.

The ability of PCDs to offer energy discrimination enhances imaging performance. A known issue with EIDs is the reduction in spatial resolution due to light spread. In contrast, PCDs exhibit relatively minor decreases in spatial resolution because of charge diffusion. Additionally, PCDs can remove noise below the energy bin threshold generated in the electronic circuit.

A well-known problem with PCDs is the incorrect counting of characteristic X-ray photons due to their escape, reabsorption, or single-photon interactions caused by the charge-sharing effect [2,3]. Optional ASIC-level anticoincidence (AC) between adjacent pixels, which sums the distributed signals and assigns them to the pixel with the highest signal, mitigates the charge-sharing effect [4].

In this study, we evaluated the imaging performance of PCDs under various exposure conditions of spectrum of 70 kV/21-mm Al filtration using quantitative metrics such as the modulation transfer function (MTF), noise power spectrum (NPS), and detective quantum efficiency (DQE).

Additionally, we discuss the cross-correlation between energy channels in relation to the AC option. Furthermore, we investigated the impact of pixel intercommunication, or the anticoincidence (AC) method, embedded in the PCD on the DQE. We also compared the DQE performance with those obtained from conventional amorphous silicon (a-Si) thin-film transistor (TFT)-based FPDs and the recent indium gallium zinc oxide (IGZO) TFT-based FPDs using the same X-ray spectrum [5].

2. Methods and Materials

2.1 PCD

The PCD used in this study was the commercial XC-TDI200 (Direct Conversion AB, Sweden). It consisted of eight small detector modules, each containing pixels with a 0.1 mm pixel pitch, resulting in an active FOV of

approximately 6.4×20.5 mm (64×2048 pixels). The sensor material was cadmium telluride (CdTe) with a thickness of 2 mm.

For dual-energy (DE) imaging, the PCD used in this study employed two energy thresholds: E_L and E_H . The low-energy image (I_L) was composed of X-ray photons with energies between E_L and E_H , while the high-energy image (I_H) corresponded to photons with energies greater than E_H . Photons with energies below E_L were discarded.

2.2 EID

The two FPDs were similar but differed in their TFT technology. The IGZO TFTs have charge carrier mobilities more than 10 times faster than those of a-Si. Additionally, the IGZO FPD operates with lower electronic noise.

The sample a-Si FPD (FDX4343R, Toshiba Co., Japan) had a 3008×3072 pixel format with a 0.143 mm pitch, while the IGZO FPD (17HQ901G-B, LG Electronics Co., Ltd., Korea) had a 3072×3072 pixel format with a 0.140 mm pitch. Both FPDs used ~ 0.5 mm-thick CsI for detecting X-ray photons.

2.3 DQE

Image quality models, such as the modulation transfer function (MTF) and noise power spectrum (NPS), have significantly influenced the development of X-ray imaging systems, particularly energy-integrating flat-panel detectors (FPDs). The combined concept of MTF and NPS, often referred to as noise-equivalent quanta (NEQ) or detective quantum efficiency (DQE), has proven to be a valuable framework for system optimization.

The DQE measurements of single-channel PCDs follow the standard methodology used for EIDs

$$DQE(u) = \frac{\bar{c}^2 T^2(u)}{\bar{q}_0 W(u)}, \quad (1)$$

Where, \bar{q}_0 , \bar{c} , $T(u)$, and $W(u)$ represent the incident X-ray photon fluence (mm^{-2}), respectively, while u denotes the spatial frequency. However, applying this formula to the DQE of multi-channel or dual-energy (DE) PCDs was unclear. Recently, a formula has been introduced that describes the DQE of multi-channel PCDs as a scaled bilinear form of channel-wise characteristic transfer functions (CTFs) for covariance between channels.

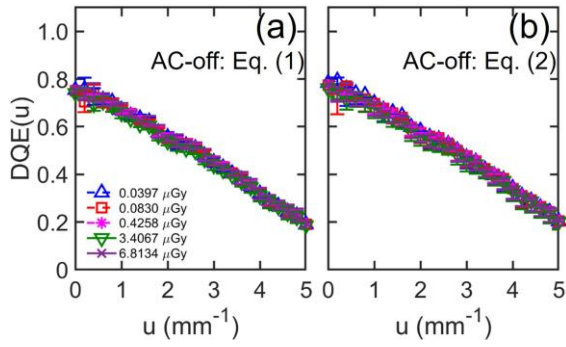


Fig. 1. Plots (a) and (b) compare the DQE curves obtained for AC-off estimated by two approaches.

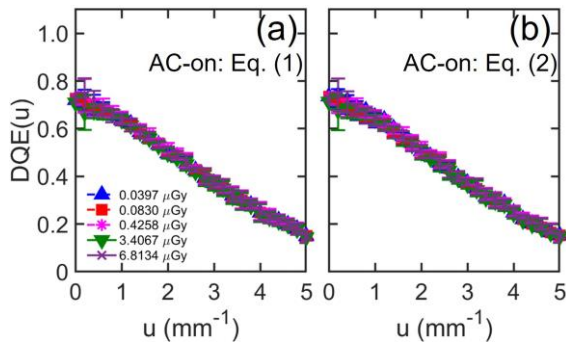


Fig. 2. Plots (a) and (b) compare the DQE curves obtained for AC-on estimated by two approaches.

$$DQE(u) = \bar{q}_0 \mathbf{f}^T \mathbf{W}^{-1} \mathbf{f}, \quad (2)$$

Where the j th channel CTF $f_j(\mathbf{u}) = \bar{g} T_j(\mathbf{u})$ and \mathbf{W} is an $n \times n$ covariance matrix for the n -channel image, $\mathbf{u} = (u, v)^T$ is the spatial frequency vector, and \bar{g} is the detector gain.

3. Preliminary Results

Figs. 1(a) and (b) show the DQE results estimated using Eqs. (1), (2) for AC-off. Similarly, Figs. 2(a) and (b) present the DQE results estimated using Eqs. (1), (2) for AC-on. The results confirmed that multi-channel DQE is equivalent to single-channel DQE, demonstrating that the DQE model in Eq. (2) effectively incorporates cross-correlation between the two energy bin images I_L and I_H . Additionally, the DQE performance of the PCD appears independent of the input air kerma.

Fig. 3(a) compares the DQE of the PCD with that of FPDs, showing that the PCD outperforms the FPDs. Fig. 2(b) compares the zero-frequency DQE performance, where both the PCD and IGZO FPD maintain $DQE(0)$ even at very low air kerma levels, while the $DQE(0)$ of the a-Si FPD drops rapidly as the air kerma decreases.

4. Conclusion

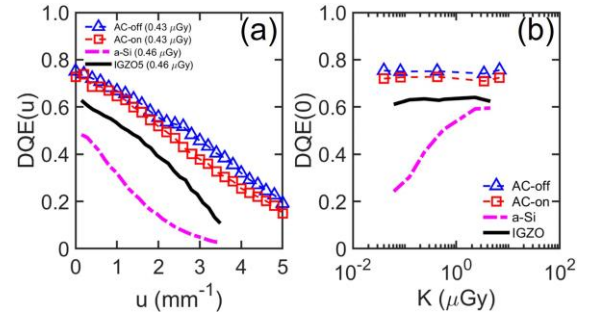


Fig. 3. Plots (a) and (b) compare the spatial-frequency-dependent DQEs and the zero-frequency DQEs with those obtained from a-Si and IGZO FPDs, respectively.

Using an X-ray spectrum of 70 kV/21-mm Al filtration, we measured the DQE of a CdTe-based DE PCD, embedding the optional AC functioning (summing the signal charges in surrounding pixels into a representative pixel). The combination of DQEs for IL and IH were equivalent to the DQE measured in the conventional way, which validates the conventional DQE form can be expanded as a sum of multi-channel DQEs. The DQE performance of the direct-conversion PCD outperformed the indirect-conversion FPDs, without degradation at the air kerma level down to 0.04 μGy . This low-dose performance was also achieved by IGZO FPD but not by a-Si FPD.

ACKNOWLEDGEMENTS

This work was conducted as a part of the research projects of "Development of automatic screening and hybrid detection system for hazardous material detecting in port container" financially (20200611) supported by the Ministry of Oceans and Fisheries, Korea.

REFERENCES

- [1] M. J. Willemink, M. Persson, A. Pourmorteza, N. J. Pelc, and D. Fleischmann, "Photon-counting CT: Technical principles and clinical prospects," *Radiology*, vol. 289, no. 2, pp. 293–312, 2018. PMID: 30179101.
- [2] J. Tanguay, J. Kim, H. K. Kim, K. Iniewski, and I. A. Cunningham, "Frequency-dependent signal and noise in spectroscopic x-ray imaging," *Med. Phys.*, vol. 47, no. 7, pp. 2881–2901, 2020.
- [3] J. Kim, J. Tanguay, I. A. Cunningham, and H. K. Kim, "X-ray interaction characteristic functions in semiconductor detectors," *J. Instrum.*, vol. 15, p. C03029, mar 2020.
- [4] K. Taguchi, "Multi-energy inter-pixel coincidence counters for charge sharing correction and compensation in photon counting detectors," *Med. Phys.*, vol. 47, no. 5, pp. 2085–2098, 2020.
- [5] S. Oh, S. Yoo, H. Shin, J. Lee, D. U. Kim, and H. K. Kim, "Signal and noise analysis of a metal oxide transistor-based flat-panel detector," *J. Instrum.*, vol. 18, p. C10016, oct 2023.